


Vanadium trimers randomly aligned along the c -axis direction in layered LiVO_2

K. Kojima , N. Katayama*, S. Tamura, M. Shiomi, and H. Sawa
 Department of Applied Physics, Nagoya University, Nagoya 464-8603, Japan



(Received 8 August 2019; published 13 December 2019)

Herein, we discuss the identification of vanadium trimers in layered LiVO_2 and its sulfide analog of LiVS_2 with two-dimensional triangular lattices. Our comprehensive structural studies using synchrotron x-ray-diffraction experiments clarified that vanadium trimers are randomly aligned along the c -axis direction in LiVO_2 , while the long-range ordering of vanadium trimers along the c -axis direction appears in LiVS_2 . Our results solve the long-standing issue of cluster patterns in LiVO_2 and provide an experimental basis for identifying the mechanism of trimer formation.

DOI: [10.1103/PhysRevB.100.235120](https://doi.org/10.1103/PhysRevB.100.235120)

I. INTRODUCTION

The entanglement of multiple electronic degrees of freedom in transition metal compounds frequently results in the spontaneous formation of clusters, called orbital molecules [1–11]. Recent structural studies have successfully clarified the complex arrangement of clusters, such as “octamers” in CuIr_2S_4 [1], “helical dimers” in MgTi_2O_4 [2], “pairs of trimers and tetramers” in AlV_2O_4 [3], and magnetic “trimerons” in Fe_3O_4 [4]. However, in layered LiVO_2 with a two-dimensional triangular lattice, the pattern of clusters has never been identified despite the intensive structural studies over a half century [12–16] since J. B. Goodenough proposed the emergence of “trimers” based on the discussion of symmetry in 1963 [17]. Nevertheless, many theoretical efforts have been devoted to clarify the mechanism of “unidentified” trimer formation [17–22], resulting in many possible scenarios including charge-density-wave instability [17,18], spin Peierls type [19], orbital ordering [20], and nesting scenarios under the synergetic effect of Coulomb interactions and trigonal-field splitting [21]. Furthermore, the recent studies using pair distribution function (PDF) analysis revealed that the disordered orbital molecules often appear in high-temperature paramagnetic phase in such systems, possibly leading to the nonequilibrium physics [10,23]. Therefore, the identification of cluster patterns in LiVO_2 has been increasingly required.

Some previous structural studies are not contradictory to the emergence of vanadium trimers in LiVO_2 . Both the vanadium K -edge x-ray-absorption fine-structure (EXAFS) and PDF show peaks which correspond to the neighboring V-V distance, which split into two peaks upon cooling below the transition temperature [13,14]. This is expected to be realized when vanadium trimers appear. Single-crystal x-ray- and electron-diffraction experiments clearly show the emergence of superstructure spots at $(1/3, 1/3, 0)$ and related positions, which is consistent with the vanadium trimer models [15,16].

It should be noted that these data do not identify the realization of vanadium trimers. In contrast to these findings, which indirectly support the emergence of trimers in the ab plane, little is known about the arrangement of cluster patterns along the c -axis direction. Previous single-crystal x-ray-diffraction studies have claimed that the superstructure peaks are accompanied by diffuse streaks along the c^* axis [15,24], which possibly indicates the absence of long-range ordering of cluster patterns along the c -axis direction. We need to consider the origin of diffuse streaks and construct a possible structural model for refinement.

Before addressing this issue, we introduce LiVS_2 , a sulfide analog of LiVO_2 , as a reference. While LiVO_2 exhibits a paramagnetic insulator to nonmagnetic insulator transition at approximately 490 K [16], LiVS_2 exhibits a metal to nonmagnetic insulator transition at approximately 314 K [8]. In LiVS_2 , on the basis of electron-diffraction and EXAFS experimental results, a trimer pattern similar to LiVO_2 is expected to be realized in a low-temperature region [8]. In contrast, the diffuse scattering along the c^* -axis direction has not been identified in LiVS_2 , with one expecting the trimer patterns to appear with a long-range ordering along the c -axis direction. Therefore, the comprehensive structural studies of both compounds should reveal the underlying factor which generates a long-range ordering of cluster patterns along the c -axis direction, leading to a complete understanding of the cluster patterns realized in low-temperature phases.

In this paper, we report vanadium trimerization, which commonly appears in low-temperature phases of LiVO_2 and LiVS_2 . While the cluster patterns are long-range along the c -axis direction in LiVS_2 , the long-range ordering is intrinsically absent in LiVO_2 . We suggest that the parent stacking structures are responsible for the absence/presence of long-range ordering of cluster patterns along the c -axis direction and propose a low-temperature structural model for LiVO_2 , which consists of three possible trimer patterns per VO_2 layer. One out of three patterns appears arbitrary in each VO_2 layer, resulting in the long-range ordering of cluster patterns being intrinsically absent along the c -axis direction in LiVO_2 . The simulated PDF pattern obtained from the structural model fits well the experimentally obtained PDF pattern at 300 K.

*katayama.naoyuki@b.mbox.nagoya-u.ac.jp

Our results successfully solve the long-standing issue of the cluster patterns of LiVO_2 , and provide an experimental basis for identifying the mechanism of trimerization.

II. EXPERIMENT

All samples were prepared according to the recipe suggested by Katayama *et al.* [8] and Tian *et al.* [16]. Our synchrotron powder x-ray-diffraction experiments clarified that the ratios of Li/V are 1.00(3) for LiVS_2 and 0.97(1) LiVO_2 , respectively. Both samples were confirmed to exhibit clear transitions at the reported temperatures using the synchrotron powder x-ray-diffraction experiment. A single-crystal x-ray-diffraction experiment was performed using R-AXIS RAPID-S (RIGAKU) equipped with a Mo target. Synchrotron powder x-ray-diffraction experiments with $E = 19$ keV were performed at the BL5S2 beamline equipped at Aichi Synchrotron, Japan. RIETAN-FP and VESTA software were employed for the Rietveld analysis and graphical purpose, respectively [25,26]. PILATUS 100 K was used for high-resolution measurement and high-speed data collection. High-energy synchrotron x-ray-diffraction experiments with $E = 61$ keV was performed for collecting the data for PDF analysis at BL04B2 at SPring-8, Japan. The hybrid detectors of Ge and CdTe were employed there. The reduced PDF $G(r)$ was obtained by the conventional Fourier transform of the collected data [27]. The PDFgui package was used for analyzing the $G(r)$ [28].

III. RESULTS AND DISCUSSION

A. X-ray diffraction analysis

Figures 1(a) and 1(b) show the single-crystal x-ray-diffraction patterns of LiVO_2 obtained at 300 K. The superstructure spots appearing at $(1/3, 1/3, 0)$, and the related positions clearly appear in Fig. 1(a). However, the superstructure spots are accompanied by diffuse streaks without any internal structures along the c^* direction, as shown in Fig. 1(b), while the fundamental peaks remain sharp. As shown in Fig. 1(c), the asymmetric broad superstructure peaks appear in the powder x-ray-diffraction data below the transition temperature, consistent with the single-crystal x-ray-diffraction results. The diffuse streaks appearing accompanied by superstructure spots indicate the absence of long-range ordering of cluster patterns along the c -axis direction in LiVO_2 .

In contrast to LiVO_2 , the prominent superstructure peaks appear for LiVS_2 below the transition temperature, as shown in the inset in Fig. 1(d). This observation indicates the presence of long-range ordering in cluster patterns along the c -axis direction in LiVS_2 . By assuming the trigonal space group $P31m$, we can successfully refine the crystal structure to obtain the low-temperature crystal structure with vanadium trimers, as shown in Figs. 1(e) and 1(f). Of note, vanadium trimerization displaces the nearest-neighboring sulfur ion upwards due to the increasing Coulomb repulsion between them, which results in an uneven buckling structure of sulfur layers on both sides of the vanadium layer, as shown in the horizontal graph in Fig. 1(f).

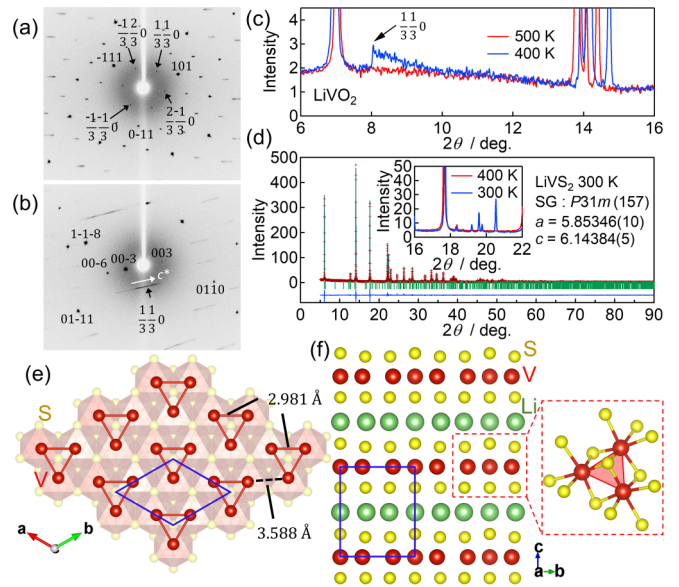


FIG. 1. (a),(b) Single-crystal x-ray-diffraction patterns of LiVO_2 at 300 K perpendicular (a) and parallel (b) to c^* direction. (c) Powder-diffraction patterns above and below the transition temperature of approximately 490 K in LiVO_2 . (d) Rietveld refinement of LiVS_2 at 300 K, assuming the space group $P31m$. The obtained reliability factors were $R_{wp} = 5.033\%$, $R_p = 4.621\%$, $R_e = 3.181\%$ and $S = 1.5821$. The inset shows powder-diffraction patterns above and below the transition temperature of 314 K. (e),(f) Obtained crystal structures of LiVS_2 at 300 K.

B. Crystallographic considerations

It is important to understand what distinguishes LiVO_2 from LiVS_2 in the absence/presence of long-range ordering of cluster patterns along the c -axis direction. Here we explain that the difference in stacking structure among them can be attributed to the absence/presence of long-range ordering. While LiVO_2 crystallizes in a $3c$ structure with $R\bar{3}m$, LiVS_2 possesses a $1c$ structure with $P\bar{3}m1$ at high temperatures. When vanadium trimers are formed in the lower layer as shown in Fig. 2(a), vanadium trimers displace the nearest-neighboring sulfur ions upwards due to the Coulomb

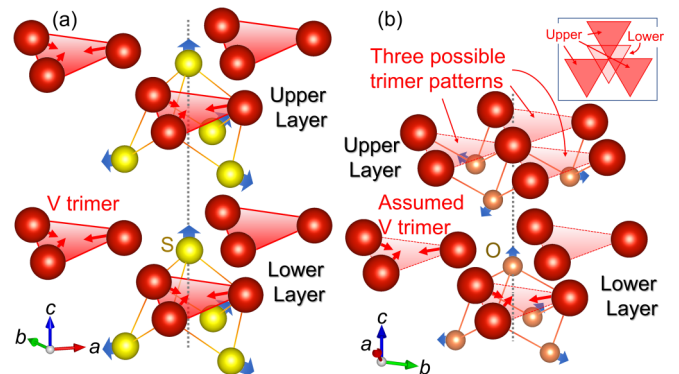


FIG. 2. Schematic pictures of the (a) experimentally identified trimer arrangements of LiVS_2 and (b) expected trimer arrangement of LiVO_2 . Inset shows the schematic picture of the trimer arrangement viewed from the c -axis direction. Li ions are not displayed for simplicity.

repulsion. The displaced sulfur ion further displaces the facing sulfur ions in the upper layer toward the inner-plane direction due to the increasing Coulomb repulsion. This causes further periodic shading of the Coulomb potential on the vanadium sites in the upper layer, which leads to the unique arrangement of vanadium trimers in the upper layer. Specifically, the long-range ordering of trimer patterns along the c -axis direction is caused by the propagation of atomic displacement accompanied by change in the Coulomb potential in LiVS_2 with a $1c$ structure. When the trimers are assumed to be realized in the lower layer of LiVO_2 with a $3c$ stacking structure as shown in Fig. 2(b), the trimers should displace the surrounding oxygen ions in a similar manner to LiVS_2 . In contrast to LiVS_2 , however, the trimer configuration in the upper layer cannot be uniformly determined in LiVO_2 because three possible trimer configurations become energetically comparable due to the inherent $3c$ structure. We expect that the possible three trimer patterns, shown in Fig. 2(b), should cause a kind of frustration, which leads to the intrinsic absence of long-range ordering along the c -axis direction in the trimer arrangements of LiVO_2 . Additional information is supplied in the Supplemental Material [29].

C. Pair Distribution Function analysis

Based on the above-mentioned discussion, we construct the possible structural model on the basis of the following three policies. First, long-ranged vanadium trimer arrangements appear in the ab plane. Second, oxygen ions are displaced

in a similar manner to sulfur ions in LiVS_2 accompanied by trimerization. Third, there are three possible trimer arrangements per VO_2 layer, as shown in the upper layer of Fig. 2(b), which results in $3^3 = 27$ possible patterns in a unit cell consisting of three VO_2 layers. One of the possible patterns is schematically shown in Fig. 3(a). Once the initial structural model is constructed, we can check the validity of the constructed model from the PDF analysis. If the above-mentioned model is correct, we can refine the reduced PDF $G(r)$ data using the average calculated patterns obtained from 27 possible trimer patterns. The refinement details and obtained parameters are summarized in the Supplemental Material.

Figure 3(b) shows the PDF analysis result of LiVO_2 in the range $1.8 \leq r(\text{\AA}) \leq 14$. The $G(r)$ pattern was obtained from the high-energy synchrotron x-ray-diffraction data collected at 300 K. It is observed that the calculated results fit the experimental data well with a small residual. However, when we expand the refined r region up to $1.8 \leq r(\text{\AA}) \leq 28$, a large residual appears in $r(\text{\AA}) \geq \sim 15$ and the reliability factor becomes worse, as shown in Fig. 3(c). This result occurs because the current model covers only the range $r(\text{\AA}) \leq \sim 14.85$, which corresponds to the thickness of three layers. In the current structural model, the trimer pattern appears in a unit cell consisting of three VO_2 layers and reappears in the neighboring three VO_2 layers due to the translational symmetry of the unit cell. This critically reduces the possible trimer patterns and makes the fitting worse in $r(\text{\AA}) \geq \sim 15$. On the basis of the above-mentioned discussion, we fitted the $G(r)$ pattern in the range $1.8 \leq r(\text{\AA}) \leq 28$, which approximately

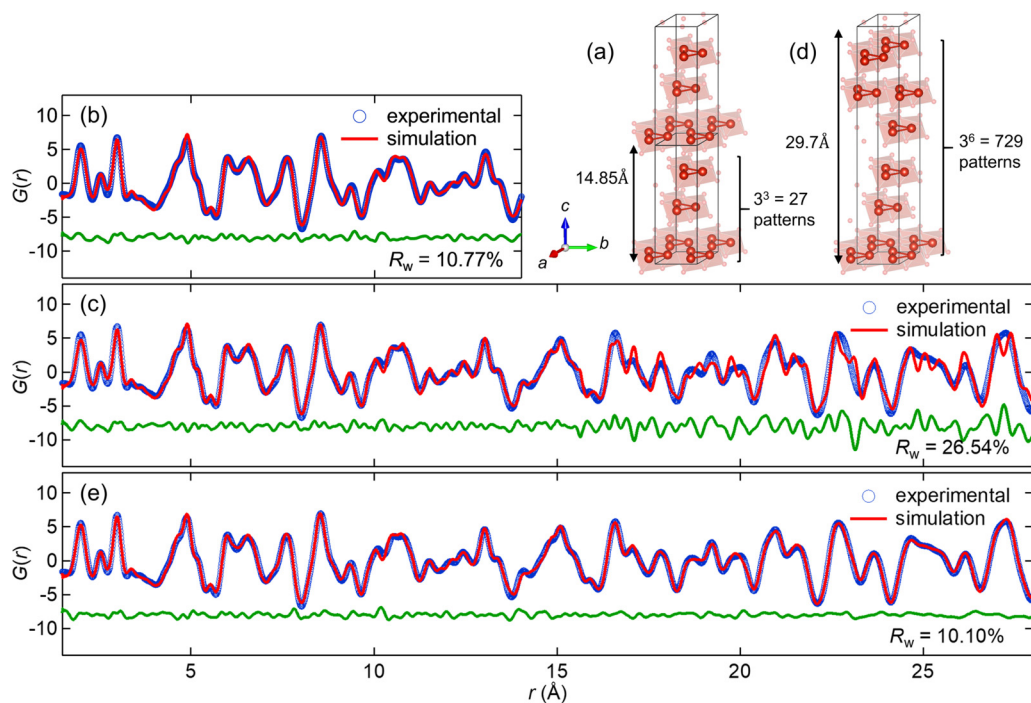


FIG. 3. (a) Schematic picture of one of the $3^3 = 27$ possible trimer patterns in a unit cell consisting of three VO_2 layers. (b),(c) Refined PDF patterns for LiVO_2 in the range of $1.8 \leq r(\text{\AA}) \leq 14$ (b) and $1.8 \leq r(\text{\AA}) \leq 28$ for (c). A simulated pattern obtained from $3^3 = 27$ possible trimer patterns was employed for the fitting. (d) Schematic picture of one of the $3^6 = 729$ possible trimer patterns in a unit cell consisting of six VO_2 layers. (e) Refined PDF patterns for LiVO_2 in the range of $1.8 \leq r(\text{\AA}) \leq 28$. A simulated pattern obtained from $3^6 = 729$ possible trimer patterns was employed for the fitting.

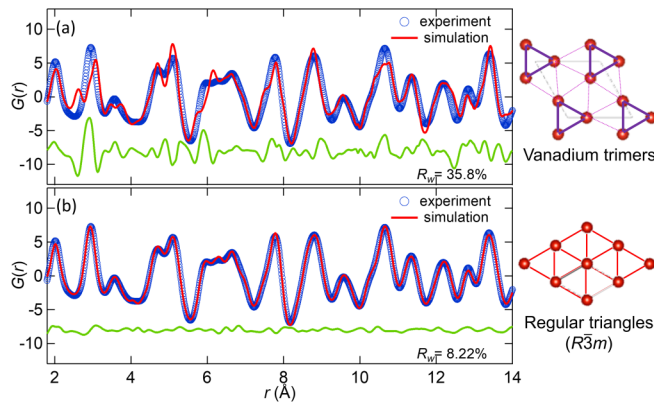


FIG. 4. (a),(b) Refined PDF patterns for LiVO_2 in the range $1.8 \leq r(\text{\AA}) \leq 14$ by assuming trimer structure (a) and regular triangle with space group $R\bar{3}m$. The data are collected at 700 K.

corresponds to the thickness of six layers, using the average calculated patterns obtained from $3^6 = 729$ possible trimer patterns, as schematically shown in Fig. 3(d). The result shows a good fit with a small residual, as shown in Fig. 3(e). The above-mentioned results clearly indicate our model of the cluster arrangements in LiVO_2 is correct, i.e., vanadium trimers crystallize in the ab plane while they are in a glassy state along the c -axis direction.

Finally, we briefly present the PDF analysis result of the high-temperature paramagnetic phase of LiVO_2 . Upon heating across the transition, the $G(r)$ pattern drastically changes. By assuming the low-temperature trimer structures, a large residual appears in the range $1.8 \leq r(\text{\AA}) \leq 14$ as shown in Fig. 4(a). In contrast, when we assume the space group $R\bar{3}m$ with a regular vanadium lattice, we successfully fit the $G(r)$ data with a small residual, as shown in Fig. 4(b). This result

indicates that the trimer molecules are disappeared at high-temperature phase of LiVO_2 .

IV. SUMMARY

Thus, our structural studies clearly solved the long-standing issue of the trimerization in LiVO_2 and show that vanadium trimers are indeed realized both in LiVO_2 and LiVS_2 . Although the mechanism of trimer formation is beyond the scope of this paper, our results provide an experimental basis for the vigorous discussion, and the obtained parameters contribute to further theoretical and experimental understanding.

ACKNOWLEDGMENTS

The authors are grateful to E. Ishii and K. Ohara for the experimental support. The work leading to these results has received funding from the Grant in Aid for Scientific Research (Grant No. JP17K17793), the Thermal and Electric Energy Technology Inc. Foundation, and the Daiko Foundation. This work was carried out under the Visiting Researcher's Program of the Institute for Solid State Physics, the University of Tokyo, and the Collaborative Research Projects of Laboratory for Materials and Structures, Institute of Innovative Research, Tokyo Institute of Technology. The synchrotron powder x-ray-diffraction experiments for Rietveld analysis were conducted at the BL5S2 of Aichi Synchrotron Radiation Center, Aichi Science and Technology Foundation, Aichi, Japan (Proposals No. 201704099, No. 201806026, No. 201804016, No. 201901018, and No. 201902056). The high-energy synchrotron powder x-ray-diffraction experiments for PDF analysis were conducted at the BL04B2 of SPring-8, Hyogo, Japan (Proposals No. 2018B1128 and No. 2018B1145).

- [1] P. G. Radaelli, Y. Horibe, M. J. Gutmann, H. Ishibashi, C. H. Chen, R. M. Ibberson, Y. Koyama, Y. S. Hor, V. Kiryukhin, and S. W. Cheong, *Nature (London)* **416**, 155 (2002).
- [2] M. Schmidt, W. Ratcliff, P. G. Radaelli, K. Refson, N. M. Harrison, and S. W. Cheong, *Phys. Rev. Lett.* **92**, 056402 (2004).
- [3] A. J. Browne, S. A. J. Kimber, and J. P. Attfield, *Phys. Rev. Mater.* **1**, 052003(R) (2017).
- [4] M. S. Senn, J. P. Wright, and J. P. Attfield, *Nature (London)* **481**, 173 (2012).
- [5] V. W. Rüdorff and H. Becker, *Z. Naturforsch. B* **9**, 614 (1954).
- [6] Y. Horibe, M. Shingu, K. Kurushima, H. Ishibashi, N. Ikeda, K. Kato, Y. Motome, N. Furukawa, S. Mori, and T. Katsufuji, *Phys. Rev. Lett.* **96**, 086406 (2006).
- [7] Y. Okamoto, S. Niitaka, M. Uchida, T. Waki, M. Takigawa, Y. Nakatsu, A. Sekiyama, S. Suga, R. Arita, and H. Takagi, *Phys. Rev. Lett.* **101**, 086404 (2008).
- [8] N. Katayama, M. Uchida, D. Hashizume, S. Niitaka, J. Matsuno, D. Matsumura, Y. Nishihata, J. Mizuki, N. Takeshita, A. Gauzzi, M. Nohara, and H. Takagi, *Phys. Rev. Lett.* **103**, 146405 (2009).
- [9] N. Katayama, S. Tamura, T. Yamaguchi, K. Sugimoto, K. Iida, T. Matsukawa, A. Hoshikawa, T. Ishigaki, S. Kobayashi, Y. Ohta, and H. Sawa, *Phys. Rev. B* **98**, 081104(R) (2018).
- [10] J. P. Attfield, *APL Mater.* **3**, 041510 (2015).
- [11] W. Tian, M. B. Stone, D. G. Mandrus, B. C. Sales, R. Jin, D. Adroja, and S. E. Nagler, *Phys. B (Amsterdam, Neth.)* **385-386**, 50 (2006).
- [12] K. Kobayashi, K. Kosuge, and S. Kachi, *Mater. Res. Bull.* **4**, 95 (1969).
- [13] K. Imai, H. Sawa, M. Koike, M. Hasegawa, and H. Takei, *J. Solid State Chem.* **114**, 184 (1995).
- [14] F. Pourpoint, X. Hua, D. S. Middlemiss, P. Adamson, D. Wang, P. G. Bruce, and C. P. Grey, *Chem. Mater.* **24**, 2880 (2012).
- [15] K. Imai, M. Koike, H. Sawa, and H. Takei, *J. Solid State Chem.* **102**, 277 (1993).
- [16] W. Tian, M. F. Chisholm, P. G. Khalifah, R. Jin, B. C. Sales, S. E. Nagler, and D. Mandrus, *Mater. Res. Bull.* **39**, 1319 (2004).
- [17] J. B. Goodenough, *Magnetism and the Chemical Bond* (Interscience and John Wiley, New York, 1963).
- [18] J. B. Goodenough, G. Dutta, and A. Manthiram, *Phys. Rev. B* **43**, 10170 (1991).

- [19] M. Onoda, T. Naka, and H. Nagasawa, *J. Phys. Soc. Jpn.* **60**, 2550 (1991).
- [20] H. F. Pen, J. van den Brink, D. I. Khomskii, and G. A. Sawatzky, *Phys. Rev. Lett.* **78**, 1323 (1997).
- [21] J. Yoshitake and Y. Motome, *J. Phys. Soc. Jpn.* **80**, 073711 (2011).
- [22] A. Subedi, *Phys. Rev. B* **95**, 214119 (2017).
- [23] S. A. J. Kimber, I. I. Mazin, J. Shen, H. O. Jeschke, S. V. Streltsov, D. N. Argyriou, R. Valentí, and D. I. Khomskii, *Phys. Rev. B* **89**, 081408(R) (2014).
- [24] M. Onoda and T. Inabe, *J. Phys. Soc. Jpn.* **62**, 2216 (1993).
- [25] F. Izumi and K. Momma, *Solid State Phenom.* **130**, 15 (2007).
- [26] K. Momma and F. Izumi, *J. Appl. Crystallogr.* **44**, 1272 (2011).
- [27] K. Ohara, S. Tominaka, H. Yamada, M. Takahashi, H. Yamaguchi, F. Utsuno, T. Umeki, A. Yao, K. Nakada, and M. Takemoto, *J. Synchrotron Radiat.* **25**, 1627 (2018).
- [28] C. L. Farrow, P. Juhas, J. W. Liu, D. Bryndin, E. S. Božzin, J. Bloch, T. Proffen, and S. J. L. Billings, *J. Phys.: Condens. Matter* **19**, 335219 (2007).
- [29] See Supplemental Material at <http://link.aps.org/supplemental/10.1103/PhysRevB.100.235120> for additional discussion about the possible trimer patterns and refinement details of LiVO_2 and LiVS_2 , with the corresponding cif files.